

## Supporting Information for

# **Native point defects modulated Cr<sup>3+</sup>-LaAlO<sub>3</sub> as in vitro excited contrast medium for in vivo near-infrared persistent deep-tissue bio- imaging**

Lu Lu<sup>a</sup>, Mingzi Sun<sup>a</sup>, Tong Wu<sup>a</sup>, Qiuyang Lu<sup>a</sup> and Bolong Huang<sup>a,\*</sup>

*<sup>a</sup>Department of Applied Biology and Chemical Technology, The Hong Kong  
Polytechnic University, Hung Hom, Kowloon, Hong Kong SAR, China*

\*E-mail: [bhuang@polyu.edu.hk](mailto:bhuang@polyu.edu.hk) (B. Huang).

## Calculation Methods

We have carried out first-principles calculations based on density functional theory (DFT) using the PBE+U level CASTEP codes<sup>1, 2</sup>. The geometry optimization has satisfied for norm-conserving pseudopotentials. To improve the accuracy of the electronic structure calculations for the defect states, the Hubbard U parameter has been induced in PBE+U calculations. For the valence states, we have chosen (5s, 5p, 5d, 6s) for La, (3s, 3p) for Al and (2s, 2p) for O, respectively. In particular, due to the atomic core-valence electron densities overlap, the OPIUM code in the Kleinman-Bylander are selected to generate the norm-conserving pseudopotential<sup>3</sup> with non-linear partial core correction<sup>4</sup> to minimize the systematic error. The RRKJ method is used for the optimization of the basis sets and ionic minimization of pseudopotentials<sup>5</sup>. To guarantee the electronic minimization and convergence, the ensemble DFT (EDFT) method of Marzari et al. has been applied to solve the Kohn-Sham equation in this work<sup>6</sup>. We have selected the ultrafine k-point sets in the Brillouin zone of LaAlO<sub>3</sub> superstructure. The geometry optimization used the Broyden-Fletcher-Goldfarb-Shannon (BFGS) algorithm through all bulk and defect supercell calculations. For all the calculations, the convergence criteria have been set as follows: (1) the total energy to under  $5.0 \times 10^{-7}$  eV per atom; (2) the Hellmann-Feynman force on each atom was converged to lower than 0.01 eV/Å.

## Supplementary Content

### 1. Oxygen vacancy in LAO

As indicated in Fig. S1, induced by oxygen vacancy defect, extra states appear in the band gap at or above Fermi level. Occupied by two electrons offered by neighboring La atoms,  $V_O^0$  gives one localized energy level within band gap. This two-electron occupied defect state locates approximately at Fermi level, 1.20 eV below the conduction band minimum (CBM). In the case of  $V_O^+$  site, only one electron is offered by nearby La. Due to the different occupancy, two split states appear in the gap, with one empty. While in  $V_O^{2+}$ , the two electrons constrained to vacancy are both ionized and this completely unoccupied defect states shift to higher energy region near CBM. The  $V_O^{2+}$  turns back to exhibit an antiferromagnetic behavior and the two empty states in opposite spin direction (spin up and down) are symmetric in band gap. The defect state of  $V_O^{2+}$  locates just 0.5 eV below the CB edge. However, the energy states of  $V_O^+$  and  $V_O^0$  are separate and localize in the upper part of band gap (0.99 eV and 1.20 eV under CBM), which can serve as deep donor. Therefore,  $V_O^+$  and  $V_O^0$  in LAO exhibit different electronic behavior from the shallow donor in other perovskite-structured oxides like  $\text{SrTiO}_3$  and  $\text{BaTiO}_3$ .<sup>7-9</sup> The trap depth of  $V_O^+$  and  $V_O^0$  are in appropriate range (0.7 eV - 1.2 eV), which suggests that they can act as efficient trapping levels for the storage of electrons to lengthen the decay time of PL.

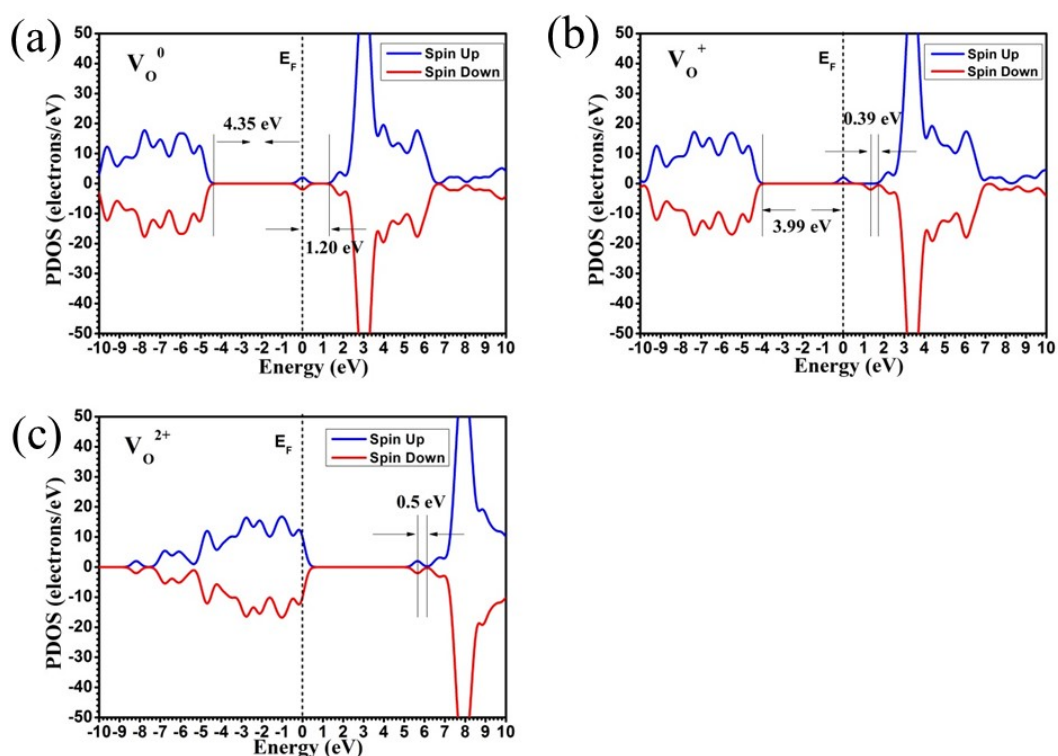


**Fig. S1.** TDOSs of O vacancy in (a) neutral ( $V_O^0$ ), (b) singly positive ( $V_O^+$ ) and (c) doubly positive ( $V_O^{2+}$ ) states. The dashed line denotes the highest occupied level for electrons.

## 2. Cation vacancies in LAO

As for Al vacancy ( $V_{Al}$ ), the bond between Al and O is broken and the unpaired electrons are remained to occupy the dangling bond of oxygen. The  $V_{Al}$  in LAO left three localized holes locating at nearby O sites. Seen from Fig. S2, one double-particle state ( $V_{Al}^-$ ) and two single-particle states ( $V_{Al}^0$  and  $V_{Al}^{2-}$ ) locate closely in the band gap. With suitable trap depth,  $V_{Al}^0$  and  $V_{Al}^{2-}$  (0.89 eV and 0.94 eV respectively) exhibit the potential to hold electrons efficiently during the trapping process. For  $V_{Al}^-$ , the double-electron occupied state locates 1.58 eV below CBM, which is too deep to act as trap levels. As for  $V_{Al}^{3-}$ , there is no defect state appearing within the band gap.

The removal of an uncharged La atom will give rise to a vacancy defect lacking three electrons. The generated holes will then be trapped by O atoms neighboring La vacancy, resulting in 0, -1, -2, and -3 charged defect states. It can be discovered from Fig. S3 that  $V_{La}^0$ ,  $V_{La}^-$  and  $V_{La}^{2-}$  generate four defect states within band gap. In the case of  $V_{La}^0$ , two localized single-particle states locate very closely in the band gap, and the interval of these two split states is about 0.74 eV. For  $V_{La}^-$  and  $V_{La}^{2-}$ , the trap depth is 1.29 eV and 0.92 eV respectively. For  $V_{La}^{3-}$ , no trap state appears within the band gap, which means that there is no hole left in LAO lattice. Since the defect states of La vacancy are predominantly contributed by La-d state, in absence of O-2p orbital, this status may forbid the electron transition without the p-d orbitals coupling.

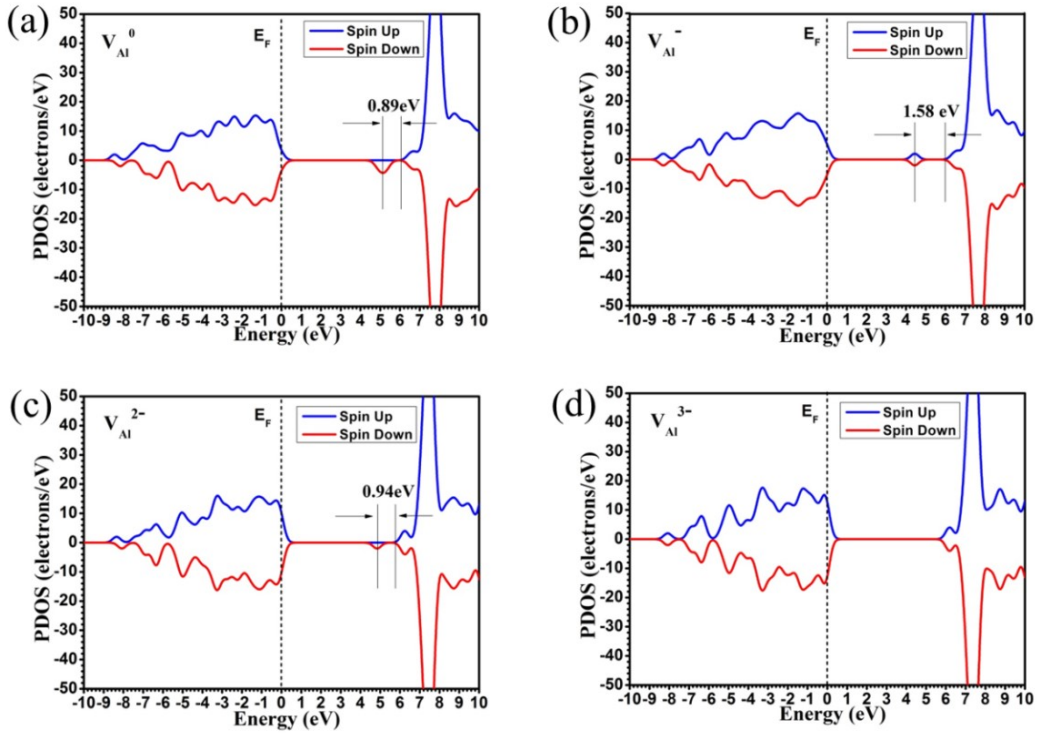


**Fig. S2.** TDOSs of Al vacancy in (a) neutral ( $V_{Al}^0$ ), (b) singly negative ( $V_{Al}^-$ ), (c) doubly negative ( $V_{Al}^{2-}$ ) and (d) triply negative ( $V_{Al}^{3-}$ ) states. The dashed line denotes the highest occupied level for electrons.

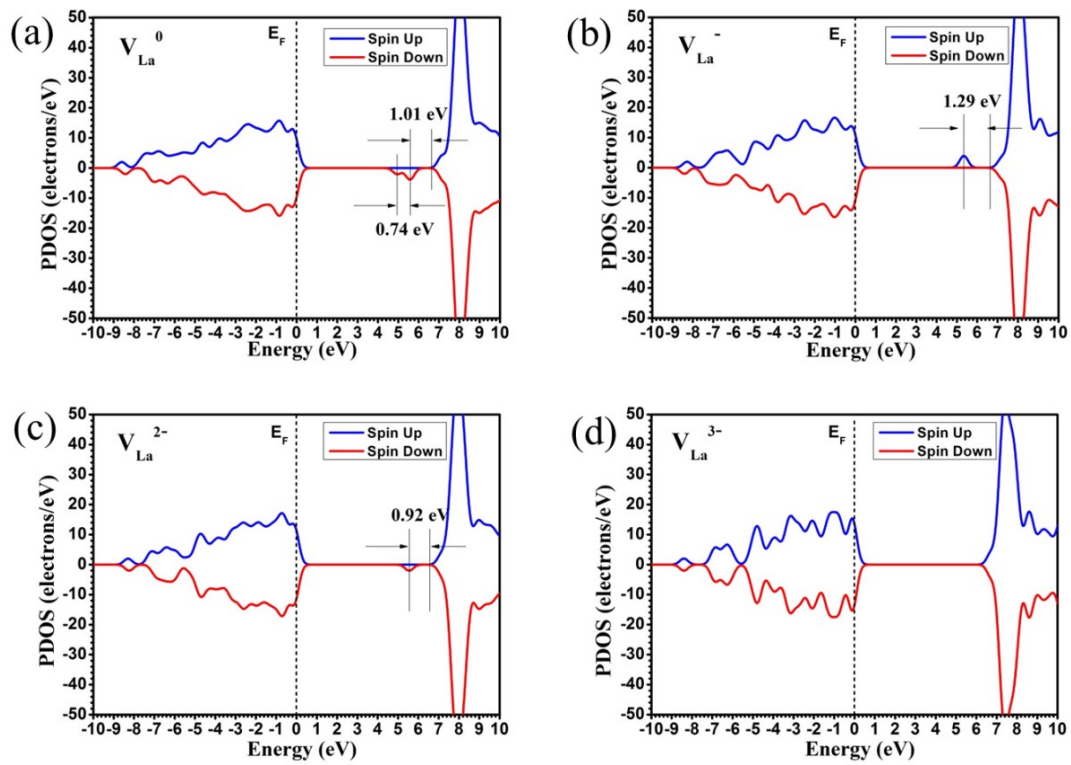


**Fig. S3.** TDOSs of La vacancy in (a) neutral ( $V_{La}^0$ ), (b) singly negative ( $V_{La}^-$ ), (c) doubly negative ( $V_{La}^{2-}$ ) and (d) triply negative ( $V_{La}^{3-}$ ) states. The dashed line denotes the highest occupied level for electrons.

### 3. Oxygen interstitial in LAO

According to the calculated TDOS in Fig. S4, there is only one localized defect state appearing within band gap for the three charged states of oxygen interstitial in LAO. For  $O_i^0$ , the two holes allow it to construct super-oxyl ion  $O_2^{2-}$  in a dumbbell-like shape with a direct O-O bond but no defect state can be discovered in band gap. As indicated in Fig. S4(b), the location of  $O_i^-$  state even touches the edge of CB, with a trap depth of 0.52 eV, which is too shallow to act as effective trap levels. The TDOS of  $O_i^-$  also demonstrates that this asymmetric state exhibits a ferromagnetic behavior. For  $O_i^{2-}$  state, it serves as a closed shell system, which is well isolated in space from other -2 charged oxygen ions. And we can see in Fig. S4(c) that there are no localized defect states appearing in the band gap.

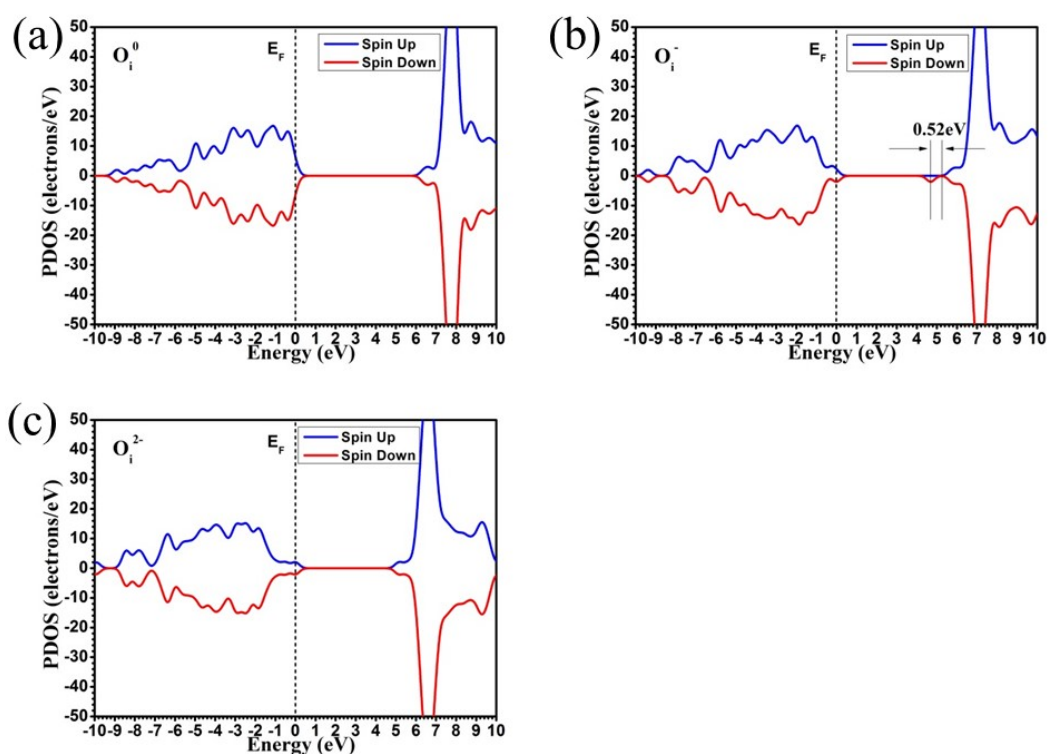


**Fig. S4.** TDOSs of O interstitial in (a) neutral ( $O_i^0$ ), (b) singly negative ( $O_i^-$ ) and (c) doubly negative ( $O_i^{2-}$ ) states. The dashed line denotes the highest occupied level for electrons.

#### 4. Cation interstitial in LAO

The interstitial Al in LAO ( $\text{Al}_i$ ) bears donor-like electrons, and the nearby O ions generate strong hybridized-bonds toward the  $\text{Al}_i$  sites. As indicated in Fig. S5, the interstitial of Al ( $\text{Al}_i$ ) totally generates five localized defect states in LAO band gap, with one asymmetry. For  $\text{Al}_i^0$ , the defect state locates 0.85 eV below CBM and the Fermi level is overlapped by conduction band (see Fig. S5a). As for  $\text{Al}_i^+$ , the defect state stands just at the Fermi level, 1.01 eV under CBM (see Fig. S5b). Fig. S5(c) shows that owing to different occupied status,  $\text{Al}_i^{2+}$  splits into two asymmetry energy states with trap depth of 1.59 eV and 0.58 eV respectively. Fig. S5(d) shows that the defect state of  $\text{Al}_i^{3+}$  is unoccupied, with an appropriate trap depth of 1.02 eV.

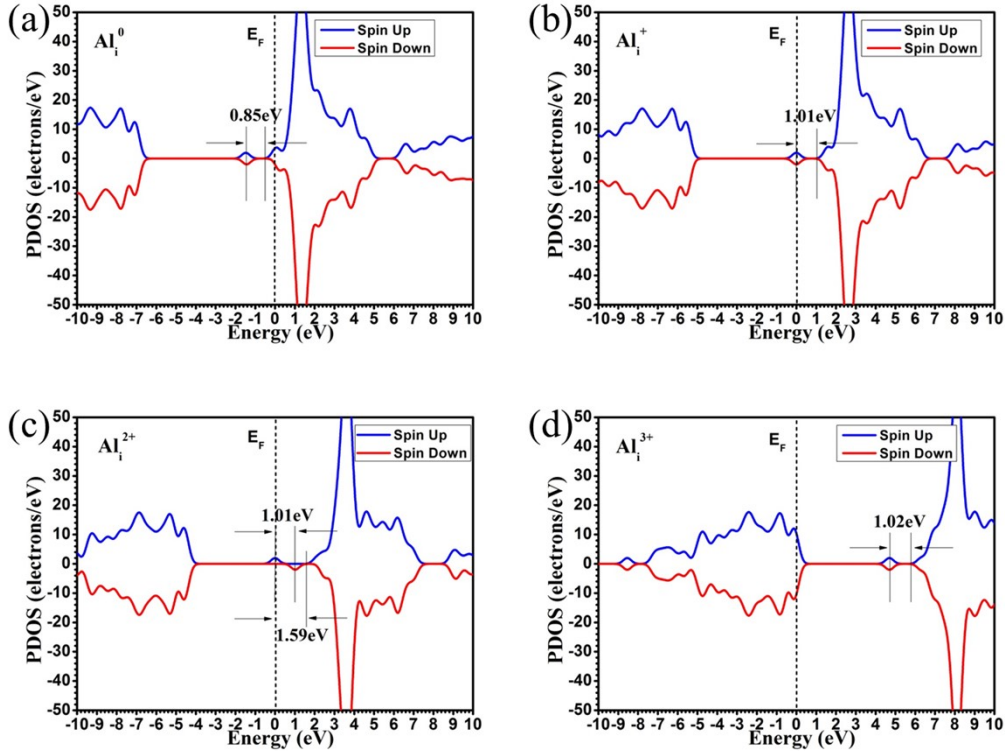


**Fig. S5.** TDOSs of Al interstitial in (a) neutral ( $\text{Al}_i^0$ ), (b) singly positive ( $\text{Al}_i^+$ ), (c) doubly positive ( $\text{Al}_i^{2+}$ ) and (d) triply positive ( $\text{Al}_i^{3+}$ ) states. The dashed line denotes the highest occupied level for electrons.

Fig. S6 indicates that the interstitial of La produces seven localized defect states within the band gap.  $\text{La}_i^0$  and  $\text{La}_i^+$  generate two defect states, 0.3 eV and 0.25 eV above VB respectively. They also produce two asymmetric shallow trap levels (occupied states) below CB, with trap depth of 0.6 eV and 0.62 eV respectively. For  $\text{La}_i^{2+}$  states, the occupied one (1.0 eV) is in suitable trap depth range, while the empty one (0.4 eV) is too shallow to trap electrons. As for  $\text{La}_i^{3+}$ , the symmetric defect state is unoccupied, located 0.84 eV below CBM.

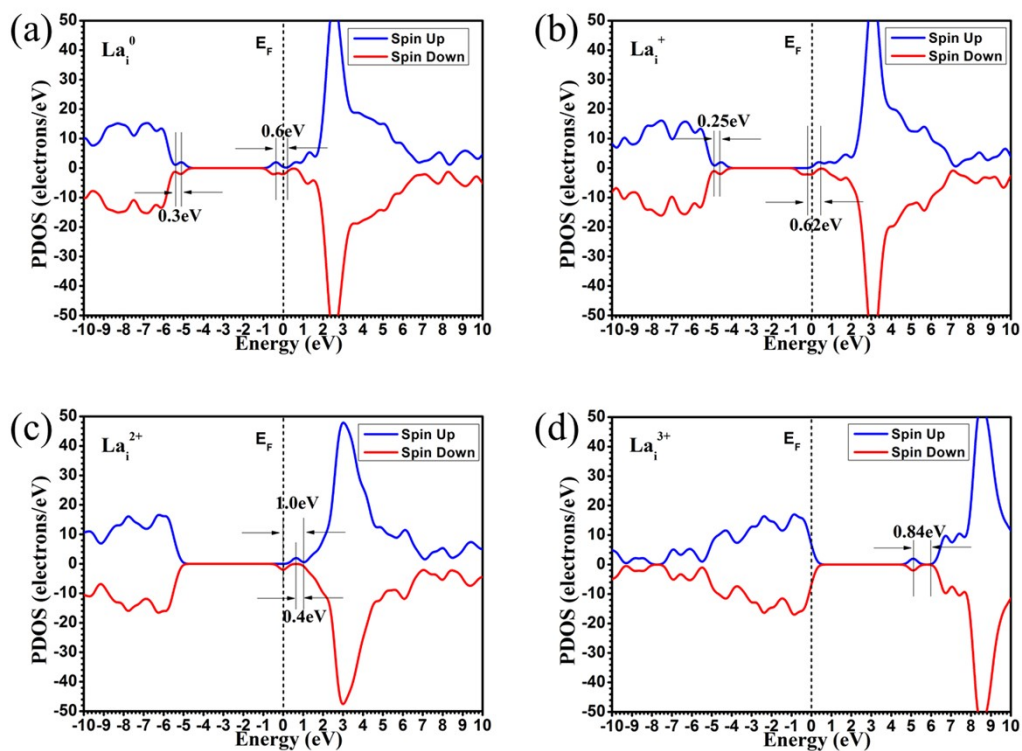


**Fig. S6.** TDOSs of La interstitial in (a) neutral ( $\text{La}_i^0$ ), (b) singly positive ( $\text{La}_i^+$ ), (c) doubly positive ( $\text{La}_i^{2+}$ ) and (d) triply positive ( $\text{La}_i^{3+}$ ) states. The dashed line denotes the highest occupied level for electrons.

## 5. Al<sub>2</sub>O<sub>3</sub> Schottky (STK) defect (V<sub>Al2O3</sub>) in LAO

STK defects are also the major native pair defects that influence the luminescent and electronic features of LaAlO<sub>3</sub>. This kind of defects are developed through nearest vacancies that accord with the stoichiometric ratio of a certain component in the host crystal, like V<sub>Al2O3</sub>, V<sub>La2O3</sub>, V<sub>AlO</sub>, V<sub>LaO</sub> and V<sub>LaAlO3</sub>. We firstly consider the situation of V<sub>Al2O3</sub> in LAO. The TDOS stimulation in Fig. S7 indicates that the defect states generated by V<sub>Al2O3</sub><sup>+</sup> (0.39 eV) and V<sub>Al2O3</sub><sup>2+</sup> (0.20 eV and 0.38 eV) are relative shallow. And one asymmetry defect state is produced by V<sub>Al2O3</sub><sup>3+</sup>, with a suitable trap depth of 0.83 eV. The trap depth of V<sub>Al2O3</sub><sup>-</sup> and V<sub>Al2O3</sub><sup>3-</sup> are 0.40 eV and 0.38 eV respectively, which are too shallow to serve as appropriate electron trapping levels. No energy state is generated by V<sub>Al2O3</sub><sup>0</sup> and V<sub>Al2O3</sub><sup>2-</sup>.

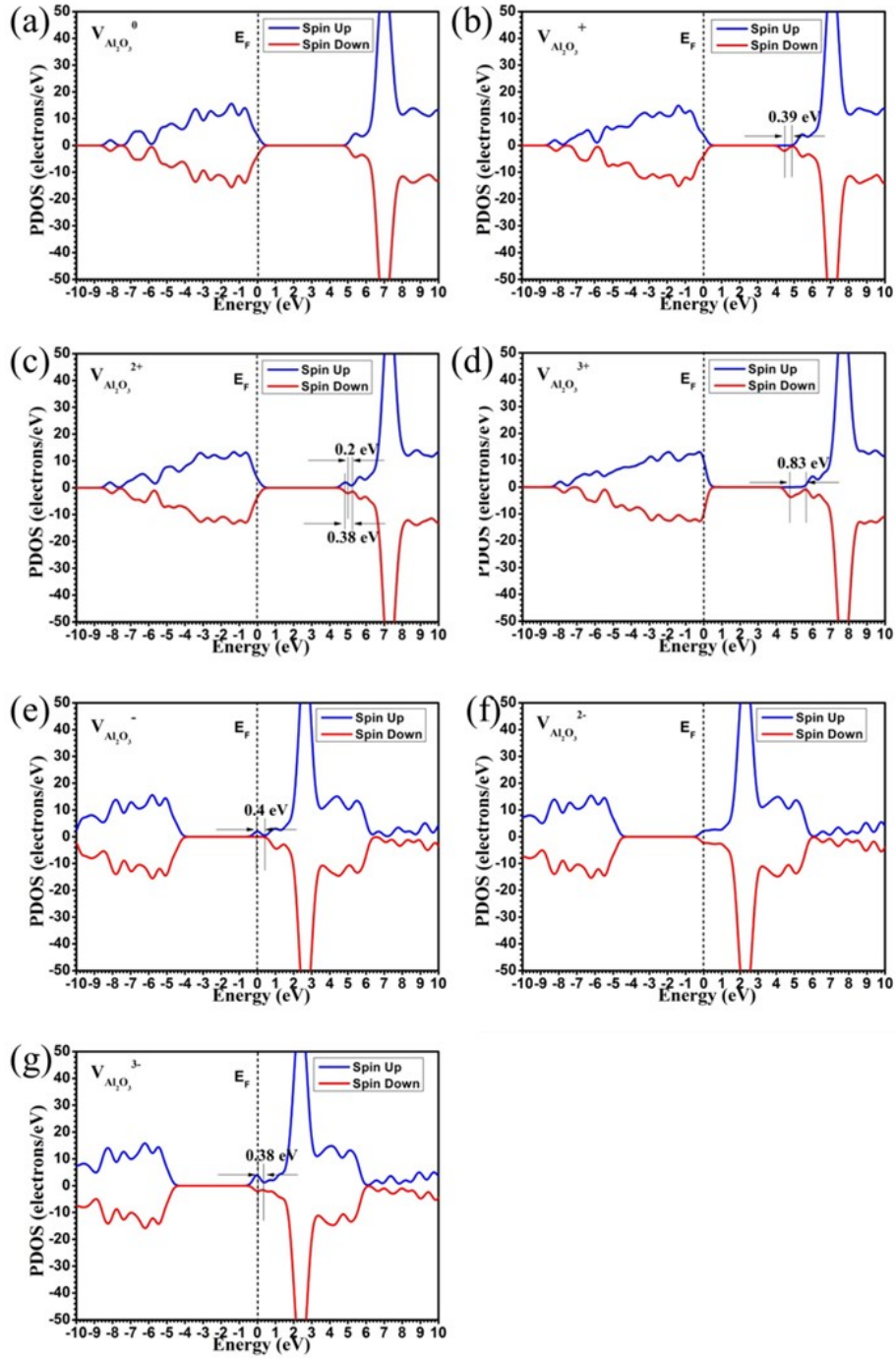


**Fig. S7.** TDOSs of  $\text{Al}_2\text{O}_3$  Schottky defect in (a) neutral ( $V_{\text{Al}_2\text{O}_3}^0$ ), (b) singly positive ( $V_{\text{Al}_2\text{O}_3}^+$ ), (c) doubly positive ( $V_{\text{Al}_2\text{O}_3}^{2+}$ ), (d) triply positive ( $V_{\text{Al}_2\text{O}_3}^{3+}$ ) (e) singly negative ( $V_{\text{Al}_2\text{O}_3}^-$ ), (f) doubly negative ( $V_{\text{Al}_2\text{O}_3}^{2-}$ ) and (g) triply negative ( $V_{\text{Al}_2\text{O}_3}^{3-}$ ) states. The dashed line denotes the highest occupied level for electrons.

## 6. $\text{La}_2\text{O}_3$ STK defect ( $V_{\text{La}_2\text{O}_3}$ ) in LAO

As illustrated in Fig. S8, the lowest defect state produced by  $V_{\text{La}_2\text{O}_3}^0$ ,  $V_{\text{La}_2\text{O}_3}^+$  and  $V_{\text{La}_2\text{O}_3}^{2+}$  are located at Fermi level, 2.2 eV, 2.38 eV and 2.43 eV away from VBM respectively. The shallow states of  $V_{\text{La}_2\text{O}_3}^0$  (0.64 eV and 0.89 eV),  $V_{\text{La}_2\text{O}_3}^+$  (1.66 eV and 0.57 eV) as well as  $V_{\text{La}_2\text{O}_3}^{2+}$  (1.27 eV and 0.3 eV) are empty and very close to the CBM. There are four localized states appearing within the band gap for  $V_{\text{La}_2\text{O}_3}^{3+}$  defect. The one-electron occupied state overlaps the Fermi level, 2.57 eV above VB. The other three are all empty, located 1.2 eV, 0.59 eV and 0.4 eV below the CBM. For  $V_{\text{La}_2\text{O}_3}^-$ , the deep state is single particle occupied, 2.05 eV above VBM. The shallow one is empty, with a trap depth of 0.87 eV. The deep energy state of  $V_{\text{La}_2\text{O}_3}^{2-}$  is double-electron occupied, situated at the Fermi level with a trap depth of 1.45 eV. The shallow one (0.5 eV) is symmetric but empty, located very close to the edge of CB. The lowest energy state of  $V_{\text{La}_2\text{O}_3}^{3-}$  locates below the Fermi level, 3.19 eV away from VBM. The one with a trap depth of 1.6 eV is single-particle occupied, standing at Fermi level. The other two are asymmetry and unoccupied, with trap depth of 0.8 eV and 0.37 eV respectively.

Among the  $V_{\text{La}_2\text{O}_3}$  deduced defect states,  $V_{\text{La}_2\text{O}_3}^0$  (0.89 eV),  $V_{\text{La}_2\text{O}_3}^{3+}$  (1.2 eV),  $V_{\text{La}_2\text{O}_3}^-$  (0.87 eV),  $V_{\text{La}_2\text{O}_3}^{3-}$  (0.8 eV) are in the range the optimal trap depth. But they are not able to hold the electrons tightly because of their unoccupied status. However, they can provide possible transition paths for the transmission of electrons which produce photon radiation in NIR-II/III biological window during the PL emission process. And the shallow levels of  $V_{\text{La}_2\text{O}_3}^0$  (0.64 eV),  $V_{\text{La}_2\text{O}_3}^+$  (0.57 eV),  $V_{\text{La}_2\text{O}_3}^{2+}$  (0.30 eV),  $V_{\text{La}_2\text{O}_3}^{3+}$  (0.40 eV and 0.59 eV),  $V_{\text{La}_2\text{O}_3}^{2-}$  (0.50 eV) and  $V_{\text{La}_2\text{O}_3}^{3-}$  (0.37 eV) are shallow trap states, which are predicted to be involved in the initial afterglow emission.

As indicated in Fig. S9, the defect states produced by AlO STK defect are all located close to the conduction band. Defect levels in  $V_{\text{AlO}}^{2-}$  and  $V_{\text{AlO}}^{3-}$  band gap are occupied states, located at the fermi level. As for  $V_{\text{AlO}}^0$ ,  $V_{\text{AlO}}^+$ ,  $V_{\text{AlO}}^{2+}$ ,  $V_{\text{AlO}}^{3+}$  and  $V_{\text{AlO}}^-$ , the valence band overlaps the fermi level, so the energy states produced by these defects are empty. The  $V_{\text{AlO}}^0$  produces two defect states within the band gap, the lower one is asymmetry while the upper one is symmetric, and the trap depth of them is 1.81 eV and 0.61 eV respectively. The two defect states produced by  $V_{\text{AlO}}^+$  are symmetric in spin status, with a trap depth of 1.18 eV (deeper one) and 0.39 eV (shallow one). In the case of  $V_{\text{AlO}}^{2+}$ , the two generated states are asymmetric (spin down), 1.0 eV and 0.21 eV below CBM. As for  $V_{\text{AlO}}^{3+}$ , two asymmetric defect states are found within the gap. The deep one is located 1.3 eV below the bottom of CB, while the shallow one is only 0.55 eV. For  $V_{\text{AlO}}^-$ , it does not generate any defect state within the host band gap. The two filled states of  $V_{\text{AlO}}^{2-}$  (single particle occupied) and  $V_{\text{AlO}}^{3-}$  (symmetric double-particle occupied) are in the range of appropriate trap depth (0.79 eV and 0.82 eV respectively) to act as electron trapping levels.

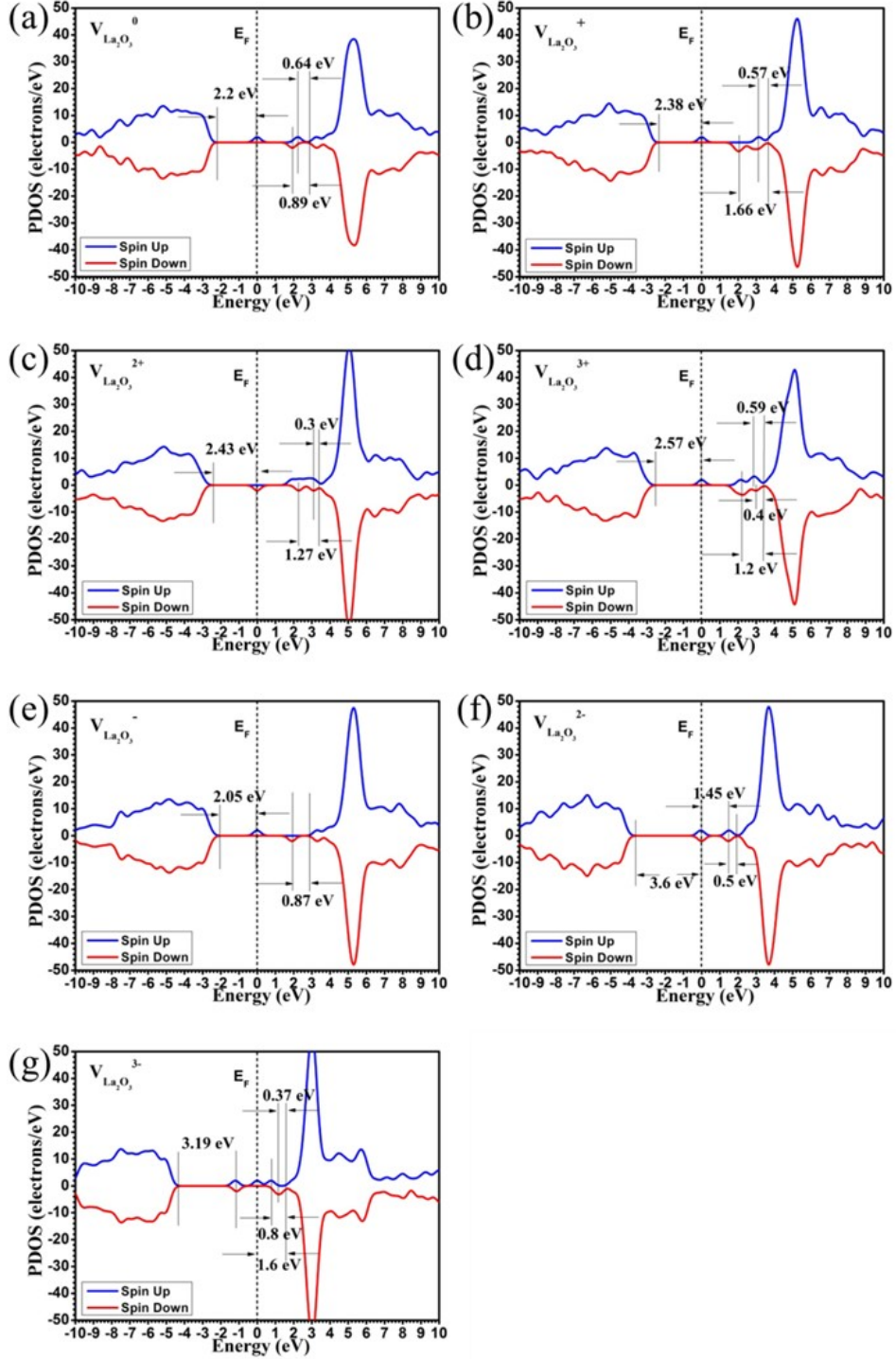


**Fig. S8.** TDOSs of La<sub>2</sub>O<sub>3</sub> Schottky defect in (a) neutral ( $V_{La_2O_3}^0$ ), (b) singly positive ( $V_{La_2O_3}^+$ ), (c) doubly positive ( $V_{La_2O_3}^{2+}$ ), (d) triply positive ( $V_{La_2O_3}^{3+}$ ) (e) singly negative ( $V_{La_2O_3}^-$ ), (f) doubly negative ( $V_{La_2O_3}^{2-}$ ) and (g) triply negative ( $V_{La_2O_3}^{3-}$ ) states. The dashed line denotes the highest occupied level for electrons.

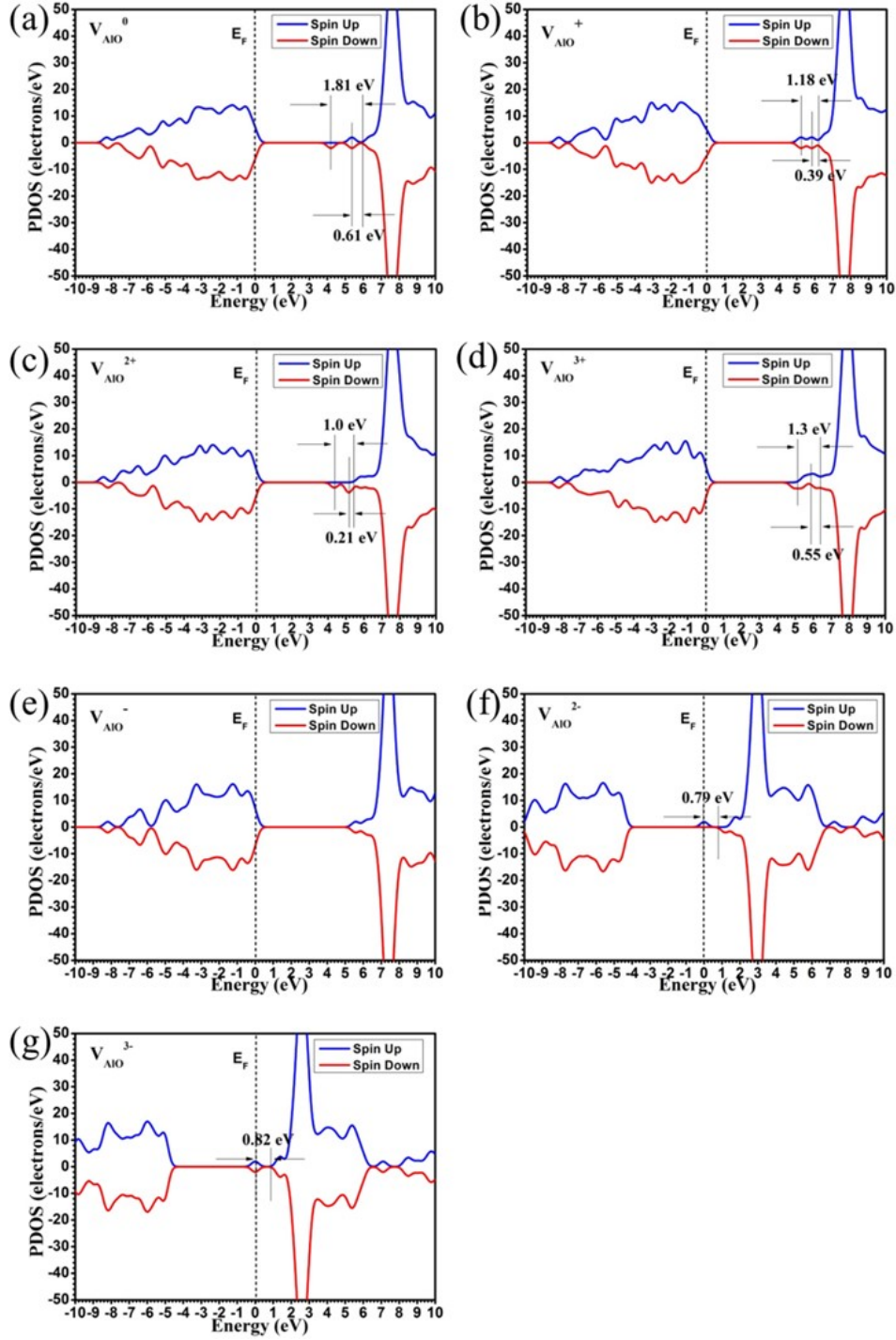


**Fig. S9.** TDOSs of AlO Schottky defect in (a) neutral ( $V_{\text{AlO}}^0$ ), (b) singly positive ( $V_{\text{AlO}}^+$ ), (c) doubly positive ( $V_{\text{AlO}}^{2+}$ ), (d) triply positive ( $V_{\text{AlO}}^{3+}$ ) (e) singly negative ( $V_{\text{AlO}}^-$ ), (f) doubly negative ( $V_{\text{AlO}}^{2-}$ ) and (g) triply negative ( $V_{\text{AlO}}^{3-}$ ) states. The dashed line denotes the highest occupied level for electrons.

## 8. LaO STK defect ( $V_{\text{LaO}}$ ) in LAO

From the TDOS data in Fig. S10, two defect states are discovered within the host band gap for  $V_{\text{LaO}}^0$ , with trap depth of 1.36 eV (asymmetric) and 0.47 eV (symmetric).  $V_{\text{LaO}}^+$  also produces two states, 1.0 eV and 0.42 eV below CBM. For  $V_{\text{LaO}}^{2+}$ , the deeper one (0.9 eV) is in suitable trap depth, and the other one (0.43 eV) is too shallow to for trapping electrons. Three defect states are generated within the band gap in the case of  $V_{\text{LaO}}^{3+}$ . Two of them are deep trapping levels, with trap depth of 1.34 eV and 1.15 eV. The shallow one is symmetric, 0.45 eV in trap depth. All of the defect states generated by  $V_{\text{LaO}}^{3+}$  are empty, located above fermi level. The defect states produced by  $V_{\text{LaO}}^-$  and  $V_{\text{LaO}}^{3-}$  are symmetric. The trap depth (0.5 eV) for the unoccupied  $V_{\text{LaO}}^-$  state is relatively shallow. As for  $V_{\text{LaO}}^{3-}$ , the state is occupied and deep, 1.3 eV away from the CBM.  $V_{\text{LaO}}^{2-}$  produces two localized states. The single-particle occupied one stands at the Fermi level, with a trap depth of 1.7 eV. While the empty one is very shallow, 0.35 eV under the CBM.

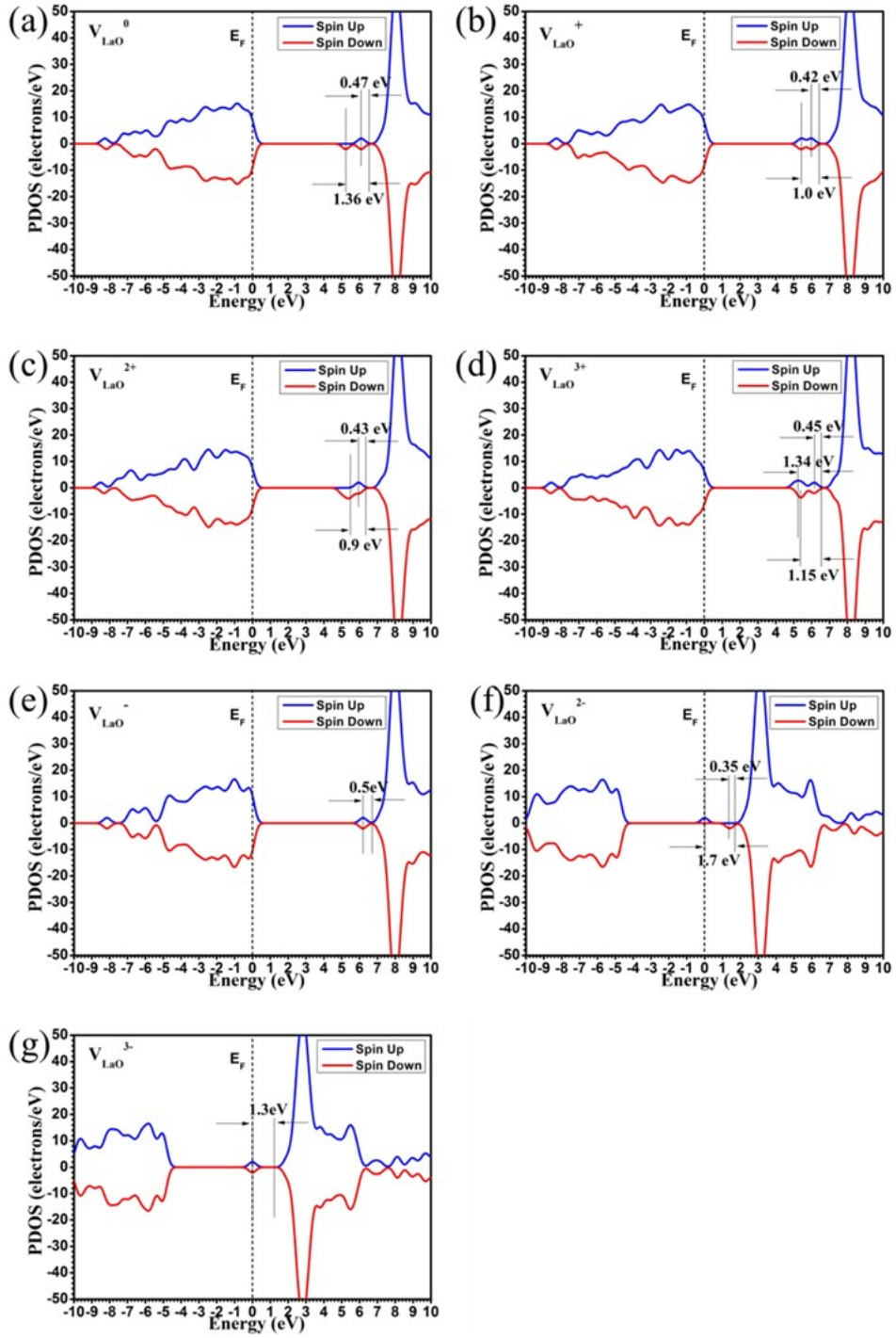


**Fig. S10.** TDOSs of LaO Schottky defect in (a) neutral ( $V_{\text{LaO}}^0$ ), (b) singly positive ( $V_{\text{LaO}}^+$ ), (c) doubly positive ( $V_{\text{LaO}}^{2+}$ ), (d) triply positive ( $V_{\text{LaO}}^{3+}$ ) (e) singly negative ( $V_{\text{LaO}}^-$ ), (f) doubly negative ( $V_{\text{LaO}}^{2-}$ ) and (g) triply negative ( $V_{\text{LaO}}^{3-}$ ) states. The dashed line denotes the highest occupied level for electrons.

## 9. $\text{LaAlO}_3$ STK defect ( $V_{\text{LaAlO}_3}$ ) in LAO

As shown in Fig. S11, the defect states generated by neutral and positive charged  $V_{\text{LaAlO}_3}$  are relatively shallower than those produced by negative charged  $\text{LaAlO}_3$  STK defect.  $V_{\text{LaAlO}_3}^0$  (0.47 eV),  $V_{\text{LaAlO}_3}^+$  (0.57 eV),  $V_{\text{LaAlO}_3}^{2+}$  (0.47 eV) as well as  $V_{\text{LaAlO}_3}^{3+}$  (0.99 eV and 0.55 eV) are located above the Fermi level. So they are all shallow empty trap states. The deep single particle occupied states of  $V_{\text{LaAlO}_3}^-$  and  $V_{\text{LaAlO}_3}^{2-}$  are located at the Fermi level, 1.8 eV and 1.86 eV away from the CBM respectively. The shallow trap states of these two STK defect types are both empty, with trap depth of 0.2 eV and 0.3 eV. In the case of  $V_{\text{LaAlO}_3}^{3-}$ , it generates three localized states (1.7 eV, 1.5 eV and 0.4 eV in trap depth) within the host band gap. The two single-particle occupied states of  $V_{\text{LaAlO}_3}^{3-}$  are deep trapping levels located below the Fermi level. The shallow one (spin up) is unoccupied and asymmetric, located very close to the CBM.

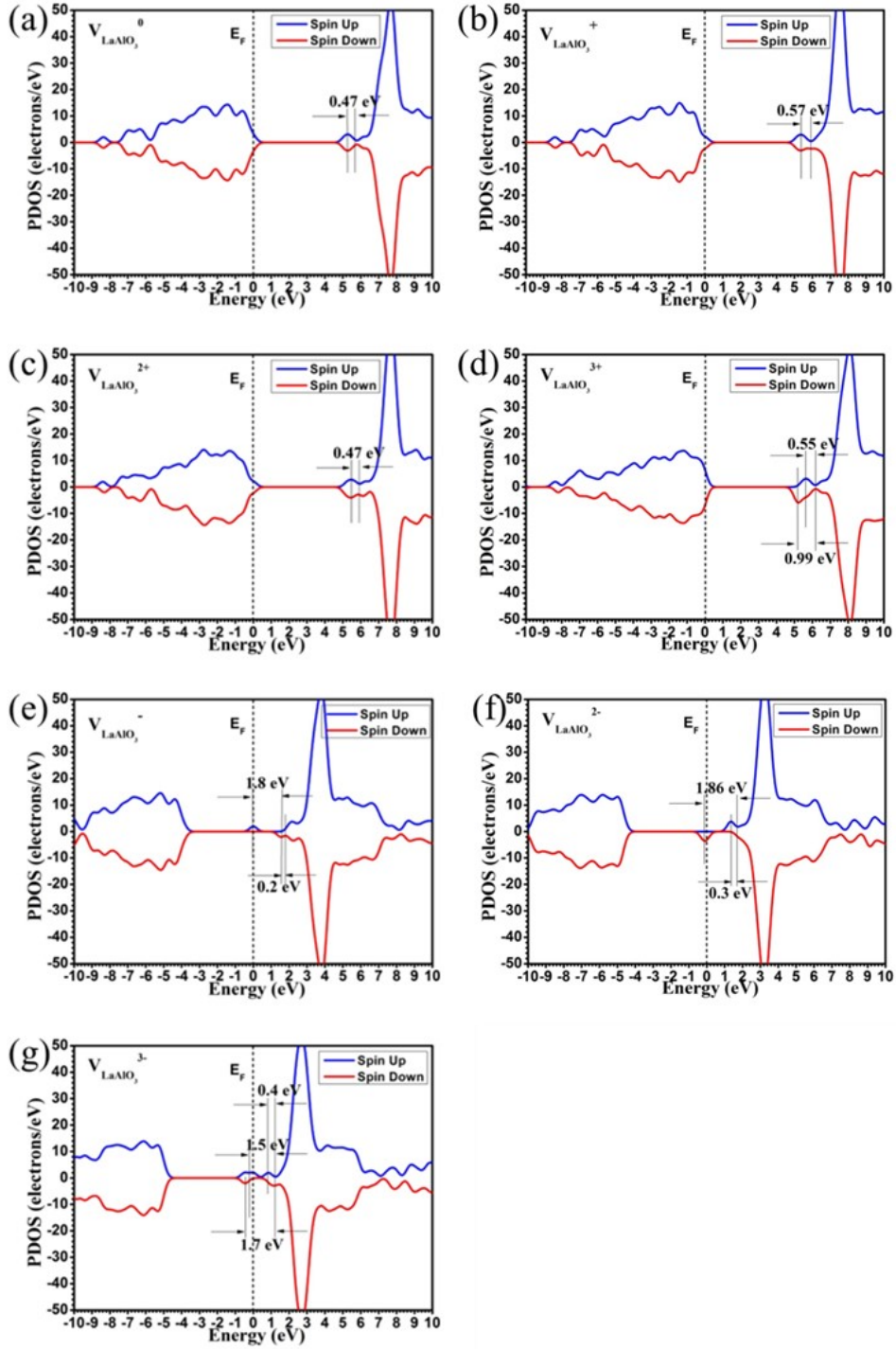


**Fig. S11.** TDOSs of  $\text{LaAlO}_3$  Schottky defect in (a) neutral ( $V_{\text{LaAlO}_3}^0$ ), (b) singly positive ( $V_{\text{LaAlO}_3}^+$ ), (c) doubly positive ( $V_{\text{LaAlO}_3}^{2+}$ ), (d) triply positive ( $V_{\text{LaAlO}_3}^{3+}$ ) (e) singly negative ( $V_{\text{LaAlO}_3}^-$ ), (f) doubly negative ( $V_{\text{LaAlO}_3}^{2-}$ ) and (g) triply negative ( $V_{\text{LaAlO}_3}^{3-}$ ) states. The dashed line denotes the highest occupied level for electrons.

## 10. Oxygen anion Frenkel pair defect (a-Fr<sub>O</sub>)

In the case of lattice distortion, we continue to investigate the charge complementary pair defects which are also the main native defects in LAO lattice. The lattice distortions are usually induced by the fluctuation of ambient conditions. We firstly deduce that the oxygen anions are perturbed and dissociated from the original host lattice and then enter into the neighbored local cage of LaAlO<sub>3</sub> motif structure. As indicated in Fig. S12, a-Fr<sub>O</sub><sup>0</sup> and a-Fr<sub>O</sub><sup>2-</sup> generate two symmetric defect states, 0.4 eV and 0.42 eV below CBM. a-Fr<sub>O</sub><sup>-</sup> produces two states in different spin status, 0.23 eV (spin down) and 0.44 eV (spin up) under the CBM respectively. The unoccupied defect state induced by a-Fr<sub>O</sub><sup>+</sup> is located in the middle of band gap, with a trap depth of 2.02 eV. No defect state is generated by a-Fr<sub>O</sub><sup>2+</sup>.

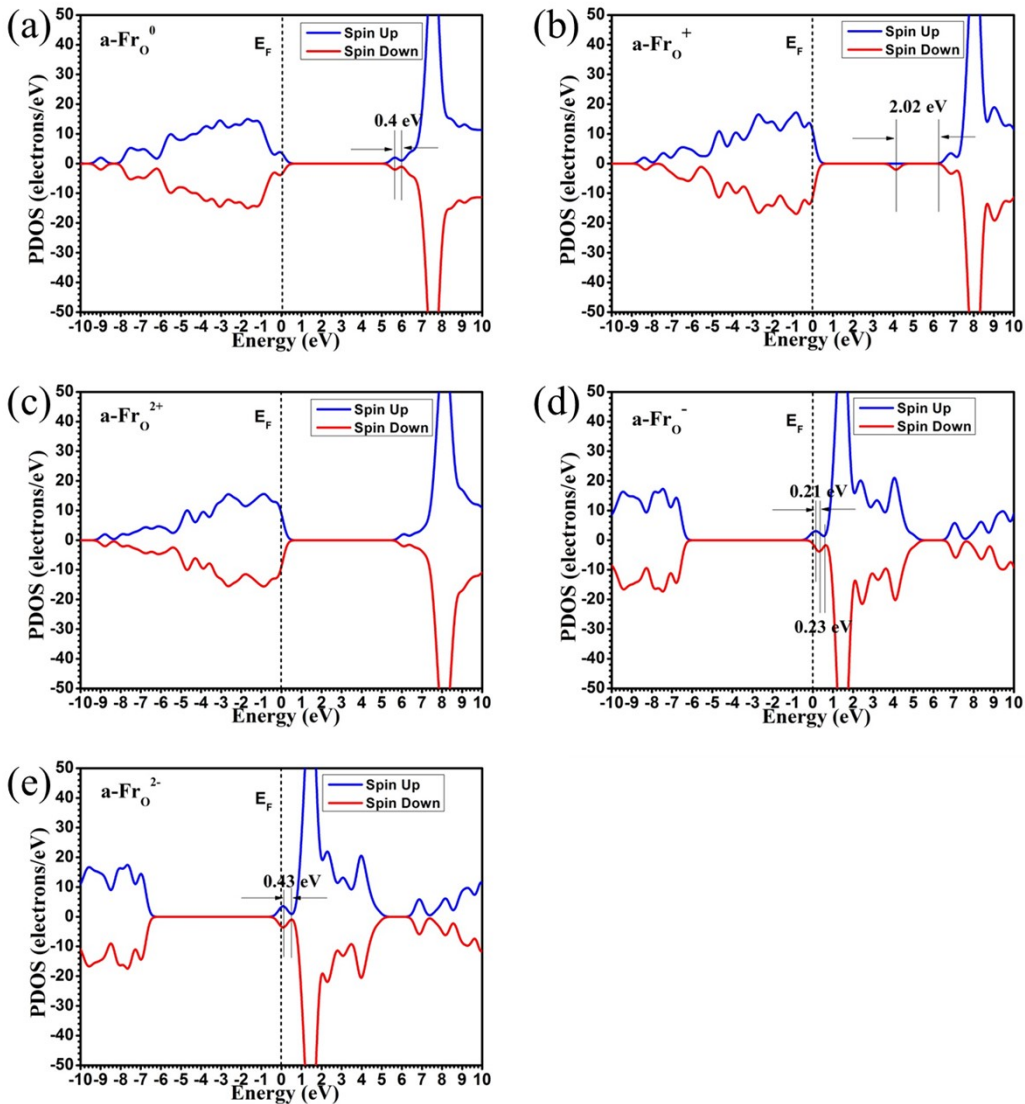


**Fig. S12.** TDOSs of oxygen anion Frenkel pair defect in (a) neutral (a-Fr<sub>O</sub><sup>0</sup>), (b) singly positive (a-Fr<sub>O</sub><sup>+</sup>), (c) doubly positive (a-Fr<sub>O</sub><sup>2+</sup>), (d) singly negative (a-Fr<sub>O</sub><sup>-</sup>) and (e) doubly negative (a-Fr<sub>O</sub><sup>2-</sup>) states. The dashed line denotes the highest occupied level for electrons.

## 11. Cation Frenkel pair defects

From the TDOS calculation in Fig. S13,  $\text{Fr}_{\text{Al}}^0$  produces one symmetric defect state (0.49 eV) next to CBM.  $\text{Fr}_{\text{Al}}^+$  generates two empty states (1.37 eV and 0.51 eV). There are three asymmetric states generated by  $\text{Fr}_{\text{Al}}^{2+}$ , 1.16 eV (spin down), 0.51 eV (spin up), 0.48 eV (spin down) under CBM respectively. The two states produced by  $\text{Fr}_{\text{Al}}^{3+}$  (0.59 eV and 0.28 eV) are relatively shallow.  $\text{Fr}_{\text{Al}}^-$  also induced two electronic states close to CB. The deep one (1.4 eV) is single particle occupied, located at Fermi level, while the shallow one (spin up) is empty, 0.4 eV below CBM. The double-particle occupied state of  $\text{Fr}_{\text{Al}}^{2-}$  is quite shallow, with a trap depth of 0.48 eV. Three single particle occupied defect states (0.39 eV, 0.78 eV and 1.09 e) are generated by  $\text{Fr}_{\text{Al}}^{3-}$ .

As indicated in Fig. S14,  $\text{Fr}_{\text{La}}^0$  does not produce any defect state within bandgap. Since the edge of VB overlaps the Fermi level in the cases of positive charged  $\text{Fr}_{\text{La}}$ , all these defect states generated are empty with shallow trap depth of 0.43 eV, 0.62 eV and 0.41 eV. The deep trap state of  $\text{Fr}_{\text{La}}^-$  is single-particle occupied, located at the Fermi level with a suitable trap depth of 1.2 eV, while the shallow one (0.45 eV) is empty. The defect states produced by  $\text{Fr}_{\text{La}}^{2-}$  (0.4 eV) and  $\text{Fr}_{\text{La}}^{3-}$  (0.55 eV) are both double-particle occupied, but they are too shallow to trap electrons tightly.

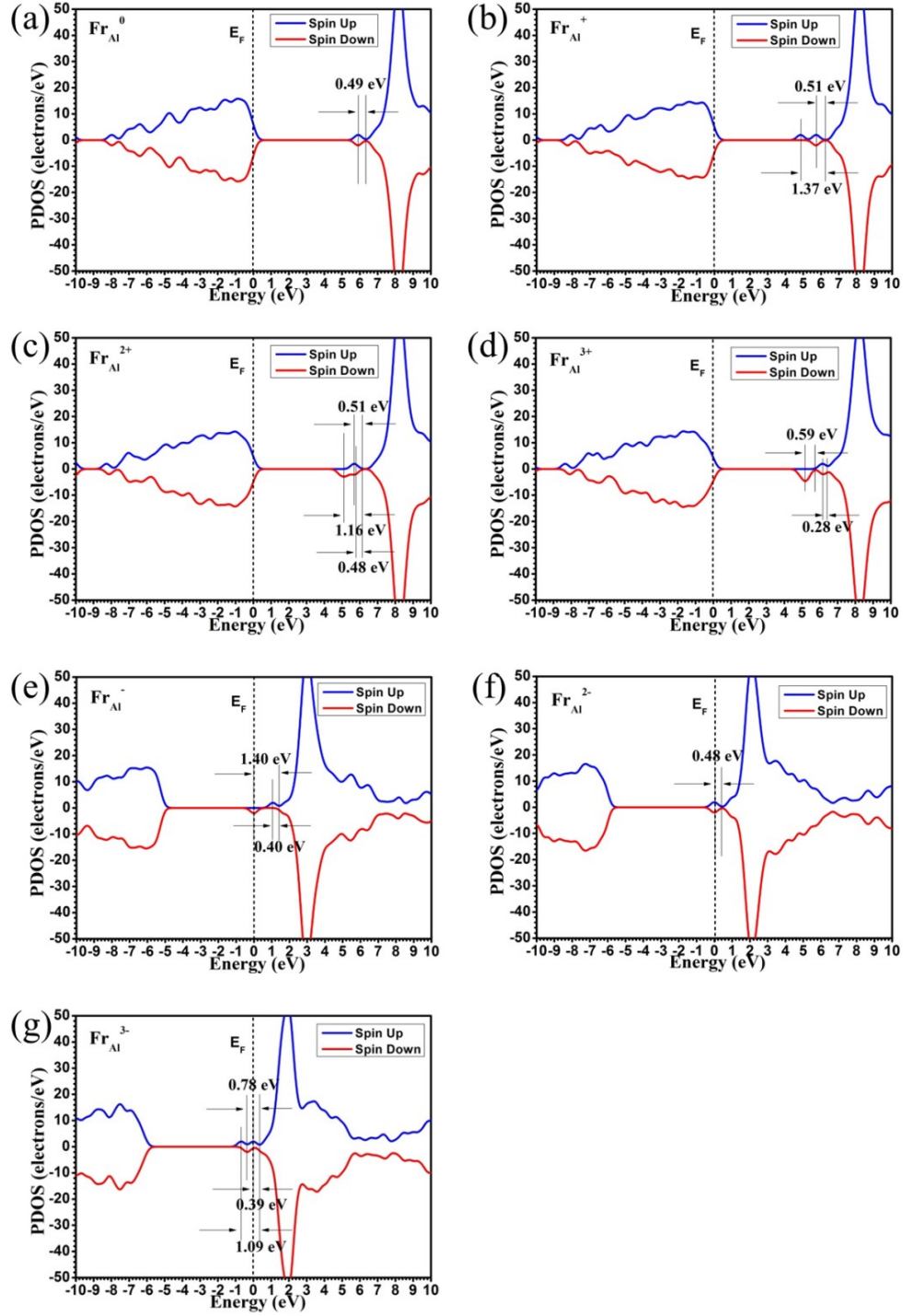


**Fig. S13.** TDOSs of Al cation Frenkel pair defects in (a) neutral ( $\text{Fr}_{\text{Al}}^0$ ), (b) singly positive ( $\text{Fr}_{\text{Al}}^+$ ), (c) doubly positive ( $\text{Fr}_{\text{Al}}^{2+}$ ), (d) triply positive ( $\text{Fr}_{\text{Al}}^{3+}$ ) (e) singly negative ( $\text{Fr}_{\text{Al}}^-$ ), (f) doubly negative ( $\text{Fr}_{\text{Al}}^{2-}$ ) and (g) triply negative ( $\text{Fr}_{\text{Al}}^{3-}$ ) states. The dashed line denotes the highest occupied level for electrons.

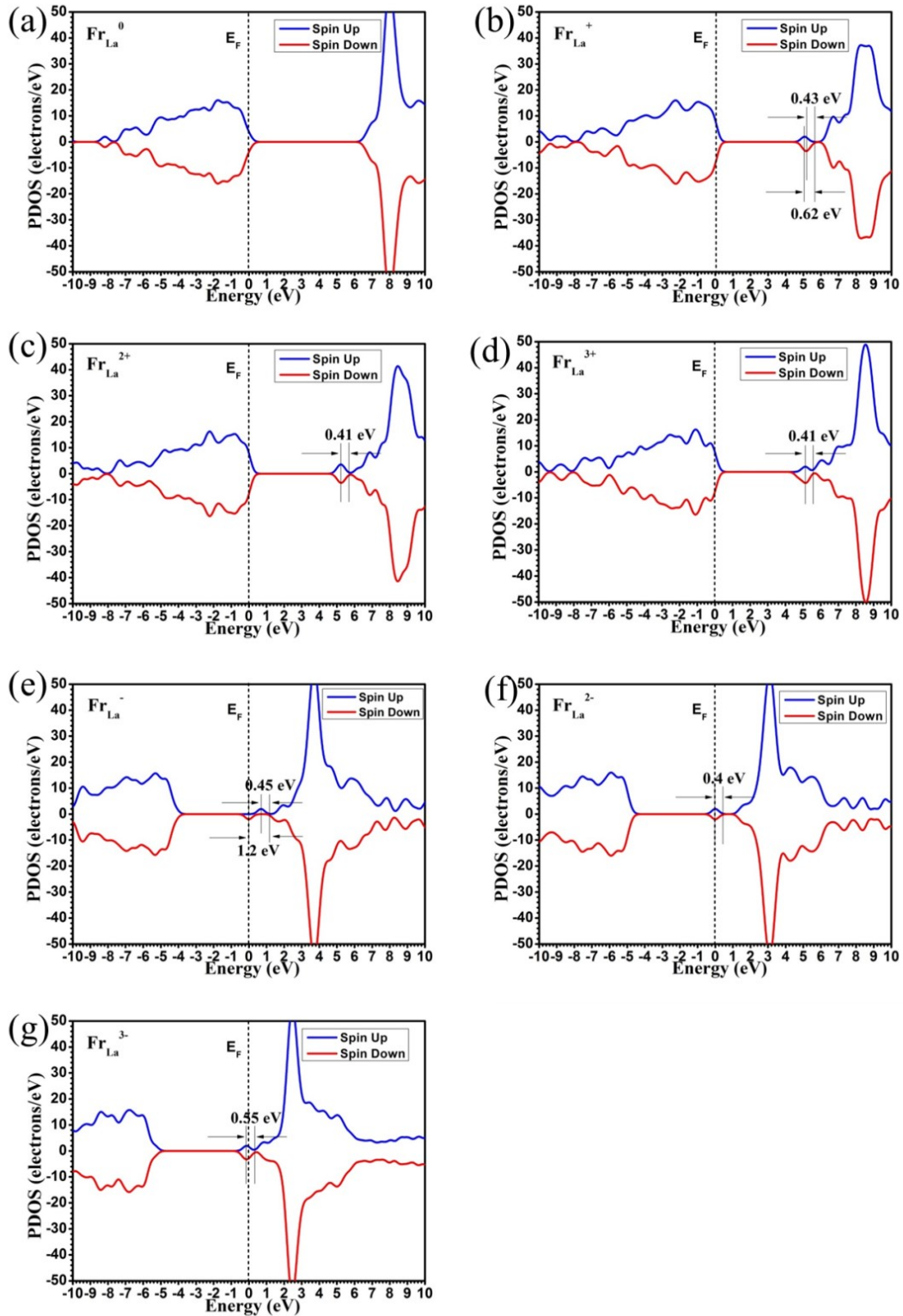


**Fig. S14.** TDOSs of La cation Frenkel pair defect in (a) neutral ( $\text{Fr}_{\text{La}}^0$ ), (b) singly positive ( $\text{Fr}_{\text{La}}^+$ ), (c) doubly positive ( $\text{Fr}_{\text{La}}^{2+}$ ), (d) triply positive ( $\text{Fr}_{\text{La}}^{3+}$ ) (e) singly negative ( $\text{Fr}_{\text{La}}^-$ ), (f) doubly negative ( $\text{Fr}_{\text{La}}^{2-}$ ) and (g) triply negative ( $\text{Fr}_{\text{La}}^{3-}$ ) states. The dashed line denotes the highest occupied level for electrons.

## Reference:

1. S. J. Clark, M. D. Segall, C. J. Pickard, P. J. Hasnip, M. J. Probert, K. Refson and M. C. Payne, *Zeitschrift Fur Kristallographie*, 2005, **220**, 567-570.
2. I. A. Vladimir, F. Aryasetiawan and A. I. Lichtenstein, *J. Phys.: Condens. Matter*, 1997, **9**, 767.
3. L. Kleinman and D. M. Bylander, *Phys. Rev. Lett.*, 1982, **48**, 1425-1428.
4. S. G. Louie, S. Froyen and M. L. Cohen, *Phys. Rev. B*, 1982, **26**, 1738-1742.
5. A. M. Rappe, K. M. Rabe, E. Kaxiras and J. D. Joannopoulos, *Physical Review B*, 1990, **41**, 1227-1230.
6. N. Marzari, D. Vanderbilt and M. C. Payne, *Phys. Rev. Lett.*, 1997, **79**, 1337-1340.
7. W.-J. Yin, S.-H. Wei, M. M. Al-Jassim and Y. Yan, *Physical Review B*, 2012, **85**.
8. M. Choi, F. Oba, Y. Kumagai and I. Tanaka, *Adv Mater*, 2013, **25**, 86-90.
9. M. Choi, F. Oba and I. Tanaka, *Applied Physics Letters*, 2011, **98**.